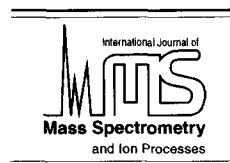




ELSEVIER

International Journal of Mass Spectrometry and Ion Processes 145 (1995) 89–96



# Negative ion formation from $\text{CH}_3\text{I}$ by electron impact

K. Nagesha<sup>1</sup>, V.R. Marathe, E. Krishnakumar\*

*Tata Institute of Fundamental Research, Homi Bhabha Road, Bombay 400 005, India*

Received 25 January 1995; accepted 23 March 1995

## Abstract

The formation of fragment negative ions from  $\text{CH}_3\text{I}$  on low energy electron collision (0–50 eV) has been measured using a pulsed electron beam and pulsed ion extraction setup in a crossed-beam geometry. In addition to  $\text{I}^-$  we have observed  $\text{H}^-$  and  $\text{CH}^-$  at specific resonant energies due to dissociative electron attachment to  $\text{CH}_3\text{I}$ . The cross-sections were put on an absolute scale using the relative flow technique. We have also carried out ab initio molecular orbital calculations to derive information on the ground state potential energy surfaces of  $\text{CH}_3\text{I}$ ,  $\text{CH}_3\text{I}^-$  and their various dissociation products.

**Keywords:** Ab initio calculations; Negative ion formation; Time of flight

## 1. Introduction

Low energy electron attachment processes, especially in the thermal and subthermal energy regions are known to play a major role in plasma chemistry [1]. Many complex molecules, and in particular polar molecules such as halogenated hydrocarbons, have large attachment cross-sections for low energy electrons and hence find applications as electron sinks in devices in which it is desired to extinguish quickly flames, plasmas or arcs. The flame-inhibiting properties of halogenated hydrocarbons are known to be due to the removal of radicals essential for flame propagation by reactions with negative

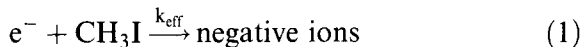
ions produced from dissociative electron attachment in the reaction zone of the flame [2]. Because of the importance of such devices in many areas of technology, molecules with large electron attachment cross-sections have attracted much attention in recent years from the point of view of various applications [3] and because of the physical basis of the attachment processes involved [4].

Low energy electron attachment to  $\text{CH}_3\text{I}$ , especially in the thermal energy region, has been studied by various workers using a variety of experimental methods such as electron swarm (ES) [5], flowing afterglow/Langmuir probe (FALP) [6], high-Rydberg beam (HRB) [7, 8], threshold photoionization (TPI) [9], and even electron cyclotron resonance (ECR) [10]. Studies on the collisions of methyl iodide with atoms in the Rydberg excited states have also been carried out [6, 8]. The rate constant  $k_{\text{eff}}$

\* Corresponding author.

<sup>1</sup> Present address: Department of Chemistry, University of Delhi, Delhi-110 007.

for the attachment process to  $\text{CH}_3\text{I}$  shown in Eq. (1) has been measured in most of these studies and has been compared by Shimamori et al. with his value of  $9.05 \pm 0.5 \text{ cm}^3 \text{ molecule}^{-1} \text{ s}^{-1}$  measured using a modified pulsed radiolysis microwave cavity method [1]:



The reaction rates of  $\text{CH}_3\text{I}$  molecules dissolved in non-polar liquids (tetramethylsilane and cyclohexane) with the electrons produced by the ionization of the solvents have been measured by Allen et al. [5,11].

In spite of the importance of electron attachment to some particular molecules discussed above, there is little information available on the quantitative assessment of these processes in terms of cross-sections for the formation of various negative ions. Spence and Schulz have measured the temperature dependence of the energy-integrated cross-sections for attachment of subthermal electrons [2]. There are no data available in the larger energy range. Further, no work has been carried out on the formation of other ions through dissociative attachment or polar dissociation of  $\text{CH}_3\text{I}$ . From this point of view we have measured the partial cross-sections for the formation of negative ions from  $\text{CH}_3\text{I}$  by electron impact using energy up to 50 eV. The measurements were carried out using a crossed-beam geometry comprising a magnetically collimated and pulsed electron beam, pulsed ion extraction and a time-of-flight mass spectrometer. The measured cross-sections were normalized to absolute values using the relative flow technique [12].

Since very little information is available on the negative ion states of  $\text{CH}_3\text{I}$ , we have performed quantum chemical calculations on neutral  $\text{CH}_3\text{I}$  and the  $\text{CH}_3\text{I}^-$  ion and their fragments (both negative ions and neutrals), in order to understand their formation, at least qualitatively, and corroborate the

energetics of the dissociative attachment process at low electron energies.

## 2. Apparatus

The arrangement of the crossed-beam apparatus we have used for the measurements has been discussed elsewhere [13]. The apparatus was designed specifically to collect, analyse and detect all the ions formed in the dissociative ionization or attachment process. In this technique, a pulsed electron beam and pulsed ion extraction technique has been employed to enable extraction of all the product ions into the time-of-flight mass spectrometer (TOFMS). The specially designed multi-element TOFMS transports all the ions entering it to the ion detector and distinguishes various ionic species according to their  $m/z$  ratio. The detection system was set for maximum and uniform sensitivity. This allows complete detection of all ions, irrespective of their mass and kinetic energies. The relative flow technique [13] was used to make the relative cross-sections absolute.

The schematic diagram of the electron collision experimental arrangement is shown in Fig. 1. This crossed-beam apparatus consists of a magnetically collimated and pulsed electron gun, a capillary array which produces the molecular beam, a pulsed ion extraction system, a Faraday cup, a multi-element TOFMS, a high resolution single flight tube TOF spectrometer and two-channel electron multipliers. Of the two TOF spectrometers, we have used the multi-element one for the present measurements. A relative flow arrangement also constitutes a part of this apparatus.

The entire electron collision arrangement was housed in a stainless steel chamber. All the materials used inside the chamber were UHV compatible. The chamber was evacuated using a combination of an ion pump and a getter pump. The lowest vacuum

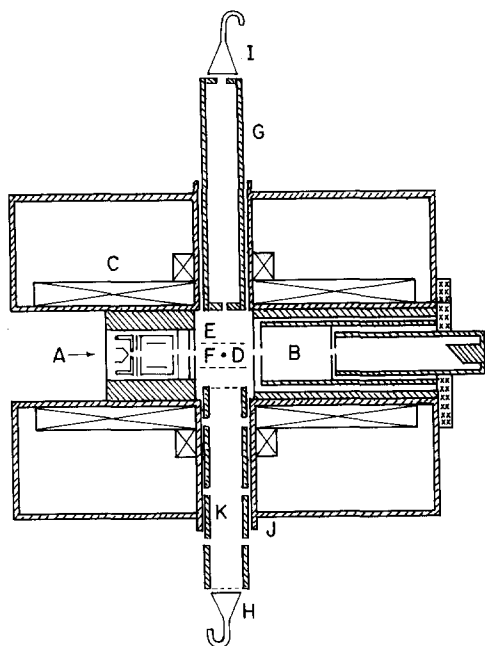


Fig. 1. Schematic diagram of the experimental arrangement: A, electron gun; B, Faraday cup; C, magnetic coils; D, capillary array; E, F, extraction grids; G, single element time-of-flight tube; H, I, channeltron detectors; J, UHV chamber for magnetic coils; K, multi-element time-of-flight lens assembly. The slanted shading represents stainless steel parts and the crossed shading represents insulator.

obtained inside the chamber was about  $3 \times 10^{-9}$  Torr. A pressure of  $\leq 1 \times 10^{-7}$  Torr was maintained during the experiments. The time difference between the electron beam pulse and arrival time of the ions at the channeltron detector was measured to generate TOF data.

The TOF spectra were taken at different electron energies to ensure proper mass resolution under the optimum conditions used for complete collection of ions. The TOF mass spectrum of  $\text{CH}_3\text{I}$  taken at an incident electron energy of 50 eV, under the optimum conditions used for complete collection of ions and proper mass resolution, is shown in Fig. 2. In addition to  $\text{I}^-$  ions, we have observed for the first time the other fragment negative ions  $\text{CH}^-$  and  $\text{H}^-$  due to electron impact on  $\text{CH}_3\text{I}$ .

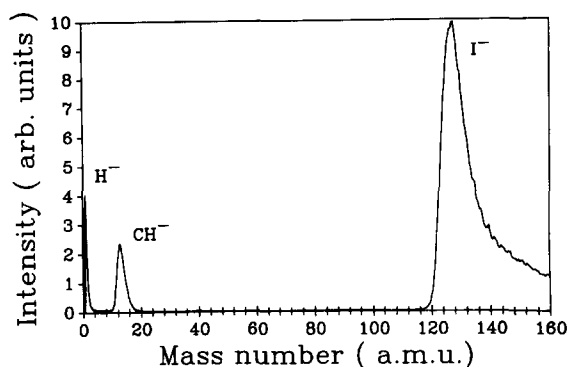


Fig. 2. The mass spectra of negative ions from  $\text{CH}_3\text{I}$  at electron energy 50 eV.

### 3. Excitation functions

The excitation function for each ion was measured by selecting specific time intervals in the time-to-amplitude converter and single-channel analyser (TAC + SCA), corresponding to each individual ion, and by scanning the electron energy in the range 0–50 eV. The energy scan was controlled by the multi-channel analyser in the multichannel scaling (MCS) mode with dwell time of 0.1 s per channel. During the entire scan the pressure of the gas behind the capillary and inside the chamber was maintained constant. The electron current was found to vary by 5–8% from 1 eV onwards. The data were corrected for this variation. The time-averaged current was about 1 nA.

In the case of  $\text{I}^-$  below 1 eV, a retarding potential method was employed to improve the energy resolution. This was possible owing to the large cross-section for the formation of these ions at very low energies.

#### 3.1. Retarding potential difference (RPD) method

The energy resolution of the primary beam of electrons obtained from the electron gun is determined mainly by the velocity distribution of the thermionic electrons constituting the

beam [14]. This resolution, which was about 0.5 eV, was not sufficient for measuring the  $I^-$  dissociative attachment resonance peak at very low electron energies. We have used the RPD method to achieve a better resolution of 0.1 eV.

The electron gun was pulsed by applying a negative voltage on the grid with respect to the Pierce element and overriding this voltage with a positive pulse of 100 ps rise time and 100 ns duration. The height of this pulse was equal to the negative d.c. voltage. In the RPD method, measurements were carried out with two settings of this d.c. and pulse amplitude. In the first case they were exactly matched in amplitude and in the second case the d.c. voltage was made further negative by 0.1 V. The difference in the data obtained in these two sets of measurements was normalized by the difference in the measured electron current to obtain the excitation function.

### 3.2. Calibration for the absolute cross-sections

The absolute cross-sections from the measured excitation functions were obtained using the relative flow technique using  $O^-$  and  $O_2$  as the standard. The expression for the unknown cross-section, in this case that of  $I^-$  from  $CH_3I$  is given by

$$\sigma\left(\frac{I^-}{CH_3I}\right) = \sigma\left(\frac{O^-}{O_2}\right) \frac{N(I^-)}{N(O^-)} \frac{F(O_2)}{F(CH_3I)} \times \frac{I_e(O_2)}{I_e(CH_3I)} \frac{K(O^-)}{K(I^-)} \sqrt{\frac{M(O_2)}{M(CH_3I)}} \quad (2)$$

where  $N$  is the number of ions collected for a specific time,  $M$  is the molecular weight of the parent molecules,  $F$  is the flow rate,  $I_e$  is the electron current,  $K$  is the detection efficiency and  $\sigma$  is the cross-section. The overall collection efficiency  $K$  in Eq. (2) is a function of the mass-to-charge ratio, and can be written as

$$K(m/z) = k_1 k_2 k_3 \quad (3)$$

where  $k_1$  is the efficiency of extraction from the ionization region,  $k_2$  is the transmission efficiency of the TOF lens assembly and  $k_3$  is the efficiency of detection of the ion by the particle detector. In practice it is difficult to isolate  $k_1$ ,  $k_2$  and  $k_3$  and one measures only  $K$ . In the present measurements, we have tried to maximize each individual efficiency by optimizing the experimental parameters [13]. The cross-section for  $O^-$  from  $O_2$  taken from Rapp and Briglia [15] is  $1.45 \times 10^{-18} \text{ cm}^2$  at the resonant peak of 6.5 eV.

### 3.3. Errors and their estimation

The possible sources of errors and their estimation have already been discussed in a similar paper [13,16]. Following that procedure, we estimate the uncertainties in the present measurements to be about 15% for incident electron energies above 1 eV. In the case of  $I^-$  below 1 eV, the RPD procedure was used for obtaining the excitation function as well as the absolute cross-section by the relative flow technique. Since the electron current below 1 eV was relatively small and also was strongly dependent on the electron energy, uncertainty in the electron current measurement was larger. The uncertainty in the electron current was further enhanced in the RPD procedure where the difference in the electron currents at two settings of the electron gun grid was used to obtain the cross-sections. We estimate the uncertainty in the measured value for the dissociative attachment peak at 0.17 eV to be 40%.

## 4. Results and discussion

The results of the measurements on  $I^-$  formation are shown in the Figs. 3(a) and 3(b). We observed a large cross-section for the formation of  $I^-$  from  $CH_3I$  at near-zero energies. The cross-section for the formation of  $I^-$  in the

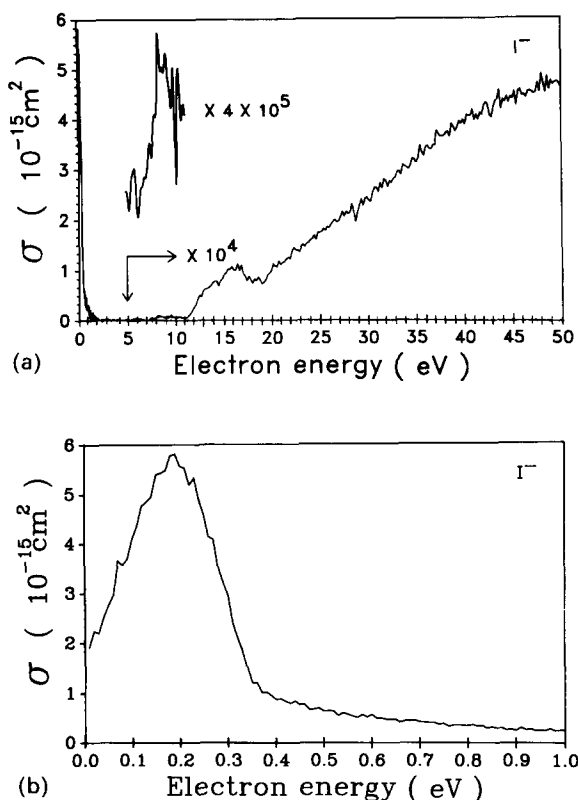


Fig. 3. The cross-section for the formation of  $\text{I}^-$  from  $\text{CH}_3\text{I}$ : (a) 0–50 eV; (b) 0–1 eV.

0–1 eV range, measured using the RPD method, is shown in Fig. 3(b). The resonance peak position for the formation of  $\text{I}^-$  was determined at 0.17 eV. Stockdale et al. [8] have determined the peak position as 0.15 eV for the  $\text{I}^-$  resonance peak, using an RPD method with an electron energy resolution of 0.1 eV. They also determined a full width at half maximum of 0.3 eV for this peak. We observed that this resonance extends up to zero electron energy. The cross-section for the formation of  $\text{I}^-$  at the 0.17 eV resonance was determined as  $5.8 \times 10^{-15} \text{ cm}^2$ . Spence et al. [2] have determined the total negative ion production cross-section from  $\text{CH}_3\text{I}$  at low energies ( $< 0.2$  eV, by integrating over the electron energy distribution rather than considering only the peak) as a function of temperature; at about 400 K the cross-section is

approx.  $5 \times 10^{-15} \text{ cm}^2 \text{ eV}$ . Since only  $\text{I}^-$  is produced from  $\text{CH}_3\text{I}$  at such low energies, this value could be compared with the area under the  $\text{I}^-$  peak measured by us which is  $2.3 \times 10^{-15} \text{ cm}^2 \text{ eV}$ . The measurements using very low energy photoelectrons [9] have given an attachment cross-section of  $3 \times 10^{-14} \text{ cm}^2$  at an energy very close to zero which falls off steadily at higher energies giving a cross-section of about  $7.5 \times 10^{-16} \text{ cm}^2$  at 150 meV. Superimposed on this relatively broad structure a smaller peak was also seen at 57 meV. The large electron attachment cross-section at near-zero energies for polar molecules, especially halogen-containing ones, has been shown to be due mostly to an s-wave scattering process in the electron/molecule interaction [4]. The above observation on  $\text{CH}_3\text{I}$  also was explained in terms of the s-wave scattering. The peak observed at 57 meV was explained as due to a second crossing of the  $\text{CH}_3\text{I}$  and  $\text{CH}_3\text{I}^-$  surfaces. The present measurements and the earlier measurements of Stockdale et al. [8], using thermionically produced electron beams, are at variance with the observation of Alajajian et al. [9]. It is likely that the relatively poor resolution in the thermionically produced electron beams is the cause of this disparity.

Apart from the peak at 0.17 eV, we have found another electron attachment peak in the  $\text{I}^-$  data at 8.6 eV with a cross-section of  $9.3 \times 10^{-21} \text{ cm}^2$ . No such peak has been reported before. Additionally, we noticed a fairly broad structure centred at 16.5 eV in the polar dissociation continuum. This corresponds to a cross-section of  $3.2 \times 10^{-19} \text{ cm}^2$ . The cross-section for the formation of  $\text{I}^-$  in the polar dissociation region is about  $10^4$  smaller than the dissociative attachment cross-section at the resonance peak at 0.17 eV. The measured cross-section at 34 eV is  $3.2 \times 10^{-19} \text{ cm}^2$ .

Apart from  $\text{I}^-$ , we also observed the formation of  $\text{H}^-$  and  $\text{CH}^-$  at particular incident electron energies. So far no other data exist

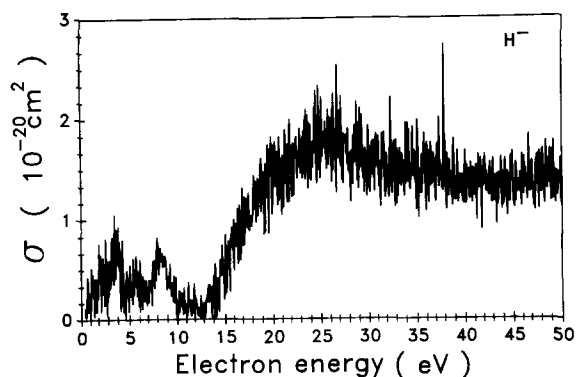


Fig. 4. The cross-section for the formation of  $\text{H}^-$  from  $\text{CH}_3\text{I}$ .

on the formation of such ions from  $\text{CH}_3\text{I}$ . The cross-sections for the formation of  $\text{H}^-$  and  $\text{CH}^-$  in the electron energy range 0–50 eV are shown in the Fig. 4 and Fig. 5 respectively. The  $\text{H}^-$  trace shows three resonance structures at 3.5 eV, 5.8 eV and 8.3 eV. The cross-sections at these resonance peak positions are  $7.5 \times 10^{-20} \text{ cm}^2$ ,  $5.0 \times 10^{-20} \text{ cm}^2$ ,  $7.0 \times 10^{-20} \text{ cm}^2$  respectively. The  $\text{CH}^-$  data show resonance structures at 3.6 and 8.4 eV with cross-sections for formation  $1.1 \times 10^{-20} \text{ cm}^2$  and  $2.62 \times 10^{-20} \text{ cm}^2$  respectively. The absolute cross-sections for  $\text{I}^-$ ,  $\text{CH}^-$  and  $\text{H}^-$  at various dissociative attachment resonance positions and at 35 eV are given in the Table 1. It is likely that the resonance formation of  $\text{H}^-$ ,  $\text{CH}^-$  and  $\text{I}^-$  around 8.5 eV occurs from the same negative ion resonance state.

We have carried out molecular orbital

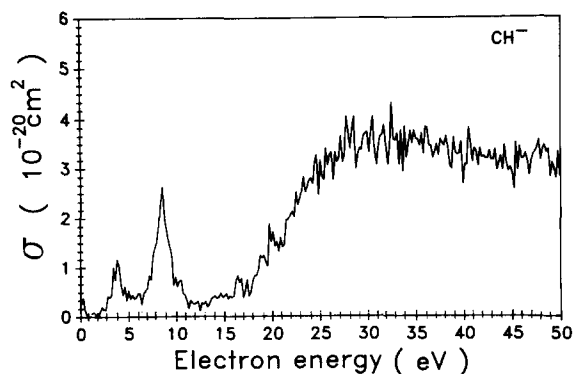


Fig. 5. The cross-section for the formation of  $\text{CH}^-$  from  $\text{CH}_3\text{I}$ .

Table 1

Cross-sections for the formation of various ions

| Ion           | Electron energy (eV) | Cross-section ( $10^{-20} \text{ cm}^2$ ) |
|---------------|----------------------|---|
| $\text{I}^-$  | 0.17                 | 580000                                    |
|               | 8.6                  | 0.93                                      |
|               | 35.0                 | 32.0                                      |
| $\text{CH}^-$ | 3.6                  | 1.1                                       |
|               | 8.4                  | 2.6                                       |
|               | 35.0                 | 31.0                                      |
| $\text{H}^-$  | 3.5                  | 7.8                                       |
|               | 5.8                  | 5.0                                       |
|               | 8.3                  | 7.0                                       |
|               | 35.0                 | 16.0                                      |

calculations on  $\text{CH}_3\text{I}$ ,  $\text{CH}_3\text{I}^-$  ion and their fragments (negative ions and neutrals) using the GAUSSIAN-90 software. For the iodine-containing species, we used the LANDLIDZ basis set [17] whereas the 6-311++G\*\* basis set was used for the other fragments. The geometry optimizations of these systems were performed using the MP2 procedure. The final energy values calculated at QCISD(T) level were used for analysing the experimental observations. The optimized geometries and corresponding energies are given in Table 2.

In Table 3 we present the electron affinities obtained using the data in Table 2 along with the existing experimental data. It is seen that the electron affinities we have obtained for H, C and I are smaller than the values given by Rosenstock et al. [18]. The difference may be attributed to the limitations of the present calculations.

$\text{CH}_3\text{I}$  has a ground state of  $^1\text{A}_1$  in the  $\text{C}_{3v}$  symmetry. We obtained optimized geometry for the ground state with C–I bond length 2.19 Å, C–H bond distance of 1.10 Å and I–C–H angle of 108.2°. These values agree fairly well with the corresponding experimental [19] values 2.132 Å, 1.084 Å and 107.68° respectively.

It was found that the ground state of  $\text{CH}_3\text{I}^-$  is not stable along the C–I bond. The Mulliken population analysis shows an effective charge

Table 2

Optimized geometries of CH<sub>3</sub>I fragments, ions and neutrals and corresponding energies, in their respective ground states

| Ion (state)                                       | Spin S | Bond distance           | (Å)    | Bond angle | (deg)  | Energy (hartree) |
|---|--------|-------------------------|--------|------------|--------|------------------|
| H   | 1/2    |                         | –      |            | –      | –0.4998179       |
| H <sup>–</sup>                                    | 0      |                         | –      |            | –      | –0.5148720       |
| C   | 1      |                         | –      |            | –      | –37.7676528      |
| C <sup>–</sup>                                    | 3/2    |                         | –      |            | –      | –37.8034881      |
| CH  | 1/2    | C–H                     | 1.118  |            | –      | –38.3914178      |
| CH <sup>–</sup>                                   | 1      | C–H                     | 1.136  |            | –      | –38.4249816      |
| CH <sub>2</sub> (C <sub>2v</sub> )                | 1      | C–H                     | 1.078  | H–C–H      | 132.7  | –39.0560107      |
| CH <sub>2</sub> <sup>–</sup> (C <sub>2v</sub> )   | 1/2    | C–H                     | 1.123  | H–C–H      | 102.4  | –39.0634956      |
| CH <sub>3</sub> (D <sub>3h</sub> )                | 1/2    | C–H                     | 1.0789 |            | –      | –39.7336808      |
| CH <sub>3</sub> <sup>–</sup> (C <sub>3v</sub> )   | 0      | C–H                     | 1.103  | H–C–H      | 109.14 | –39.7221326      |
| I   | 1/2    |                         | –      |            | –      | –11.1677618      |
| I <sup>–</sup>                                    | 0      |                         | –      |            | –      | –11.2506489      |
| CH <sub>3</sub> I (C <sub>3v</sub> )              | 0      | C–H                     | 1.10   | I–C–H      | 108.2  | –50.8887520      |
|   |        | I–C                     | 2.19   |            |        |                  |
| CH <sub>3</sub> I <sup>–</sup> (C <sub>3v</sub> ) | 1/2    | Unstable along I–C bond |        |            |        |                  |

on I to be –0.99. Thus this state is most likely to dissociate into CH<sub>3</sub> and I<sup>–</sup>. This also means that CH<sub>2</sub>I<sup>–</sup>, CHI<sup>–</sup>, or CI<sup>–</sup> ions are unlikely to be observed through dissociative electron attachment with CH<sub>3</sub>I. The Franck–Condon transition energy from the ground state of CH<sub>3</sub>I to the ground state <sup>2</sup>A<sub>1</sub> of CH<sub>3</sub>I<sup>–</sup> was calculated to be 2.30 eV. However, this does not correspond to any of the experimentally determined resonance energies.

So far there exist no calculations on CH<sup>–</sup>, CH<sub>2</sub><sup>–</sup> and CH<sub>3</sub><sup>–</sup> ions. Our calculations (Table 3) show that the CH<sub>3</sub> fragment has an electron affinity of –0.31 eV and hence cannot be experimentally observed. The value reported so far gives a positive electron affinity of 1.8 eV [18]. CH<sub>2</sub> was found to have an electron

affinity of 0.20 eV. The ground state of CH<sub>2</sub><sup>–</sup> was found to be stable against dissociation to CH + H<sup>–</sup> by 4.62 eV, suggesting that CH<sub>2</sub><sup>–</sup> could be experimentally observed. However, we have not been able to observe it in the present measurements. The minimum in the <sup>3</sup>Σ ground state of CH<sup>–</sup> was found 0.91 eV below the <sup>2</sup>Π ground state of CH. A number of values ranging from 0.74 to 4.1 eV have been reported for its electron affinity [18]. The dissociation energy of CH<sup>–</sup> was found to be 1.16 eV.

## 5. Conclusion

Absolute cross-sections for the formation of various ions from the electron attachment to CH<sub>3</sub>I have been measured in the electron energy range 0–50 eV. Electron attachment to CH<sub>3</sub>I led to the formation of I<sup>–</sup>, H<sup>–</sup> and CH<sup>–</sup> ions, which were observed at specific resonance energies. We have observed for the first time the formation of CH<sup>–</sup> and H<sup>–</sup> from CH<sub>3</sub>I and measured the cross-sections for their formation.

The results of the ab initio molecular orbital calculations performed on these negative

Table 3

The calculated electron affinities of various species and existing experimental data

| Species         | Calculated electron affinity (eV) | Range of measured [18] electron affinities (eV) |
|-----------------|-----------------------------------|---|
| H               | 0.41                              | 0.754–0.776                                     |
| C               | 0.97                              | 1.17–1.38                                       |
| I               | 2.25                              | 3.06–3.13                                       |
| CH              | 0.91                              | 0.74–4.1  |
| CH <sub>2</sub> | 0.20                              | –   |
| CH <sub>3</sub> | –0.31                             | 1.8   |

molecular ions show that the ground state of  $\text{CH}_3\text{I}^-$  is not stable against dissociation. The electron affinities of CH and  $\text{CH}_2$  were found to be positive whereas that of  $\text{CH}_3$  was found to be negative.

## References

- [1] H. Shimamori, Y. Tatsumi, Y. Ogawa and T. Sunagawa, *Chem. Phys. Lett.*, 194 (1992) 223.
- [2] D. Spence and G.J. Schulz, *J. Chem. Phys.*, 58(5) (1973) 1800.
- [3] Christophorou L.G., *Electron–molecule interactions and their applications*, vol. 2, Chapter 6, Academic Press, 1984.
- [4] Chutjian A., in W.R. MacGillivray, I.E. McCarthy and M.C. Standage (Eds.), *Electronic and atomic collisions, Invited Papers, VII Int. Conf. The Physics of Electronic and Atomic Collisions, Australia, July 1991*, p. 127.
- [5] L.G. Christophorou, *Chem. Rev.*, 76 (1976) 409.
- [6] E. Alge, N.G. Adams and K.A. Smith, *J. Phys. B*, 17 (1984) 3827.
- [7] G.F. Hilderbrandt, F.G. Kellert, F.B. Dunning, K.A. Smith and R.F. Stebbings, *J. Chem. Phys.*, 68 (1978) 1349.
- [8] J.A.D. Stockdale, F.J. Davis, R.N. Compton and C.E. Klotz, *J. Chem. Phys.* 60 (1974) 4279.
- [9] S.H. Alajajian, M.T. Bernius and A. Chutjian, *J. Phys. B*, 21 (1988) 4021.
- [10] A.A. Christodoulides, E. Shultes, R. Schumacher and R.N. Schindler, *Z. Naturforsch., Teil A*, 29 (1974) 389.
- [11] A.O. Allen and R.A. Holroyd, *J. Phys. Chem.*, 78 (1973) 796.
- [12] S.K. Srivastava, A. Chutjian and S. Trajmar, *J. Chem. Phys.*, 63 (1975) 2659.
- [13] E. Krishnakumar and K. Nagesha, *J. Phys. B*, 25 (1992) 1645.
- [14] J.A. Simpson, *Rev. Sci. Instrum.*, 32(12) (1961) 1283.
- [15] D. Rapp and D.D. Briglia, *J. Chem. Phys.*, 43 (1965) 1480.
- [16] E. Krishnakumar and S.K. Srivastava, *Phys. Rev. A*, 41 (1990) 2445.
- [17] P.J. Hay and W.R. Wadt, *J. Chem. Phys.*, 82 (1985) 270, 284 and 299.
- [18] H.M. Rosenstock, K. Draxl, B.W. Steiner and J.T. Herron, *J. Phys. Chem. Ref. Data*, 6 (1977) 1.
- [19] W.J. Hehre, L. Radom, V.R. Paul Schleyer and J.A. Pople *Ab Initio Molecular Orbital Theory*, Wiley, 1986.